IOP Publishing | Institute of Physics and Engineering in Medicine Physiological Measurement

Physiol. Meas. **35** (2014) 985–996 doi:10.1088/0967-3334/35/6/985

Magnetic resonance electrical impedance tomography for measuring electrical conductivity during electroporation

M Kranjc[1], F Bajd[2], I Serša[2,3] and D Miklavčič[1]

[1] Faculty of Electrical Engineering, University of Ljubljana, Tržaška 25, SI-1000 Ljubljana, Slovenia
[2] Institut 'Jozef Stefan', Jamova cesta 39, SI-1000 Ljubljana, Slovenia
[3] Department of Biomedical Engineering, Kyung Hee University, 1 Seocheon-dong, Giheung-gu, Yongin-si, Gyeonggi-do 446-701, Korea

E-mail: damijan.miklavcic@fe.uni-lj.si

Received 28 November 2013, revised 3 February 2014
Accepted for publication 17 February 2014
Published 20 May 2014

Abstract

The electroporation effect on tissue can be assessed by measurement of electrical properties of the tissue undergoing electroporation. The most prominent techniques for measuring electrical properties of electroporated tissues have been voltage–current measurement of applied pulses and electrical impedance tomography (EIT). However, the electrical conductivity of tissue assessed by means of voltage–current measurement was lacking in information on tissue heterogeneity, while EIT requires numerous additional electrodes and produces results with low spatial resolution and high noise. Magnetic resonance EIT (MREIT) is similar to EIT, as it is also used for reconstruction of conductivity images, though voltage and current measurements are not limited to the boundaries in MREIT, hence it yields conductivity images with better spatial resolution. The aim of this study was to investigate and demonstrate the feasibility of the MREIT technique for assessment of conductivity images of tissues undergoing electroporation. Two objects were investigated: agar phantoms and *ex vivo* liver tissue. As expected, no significant change of electrical conductivity was detected in agar phantoms exposed to pulses of all used amplitudes, while a considerable increase of conductivity was measured in liver tissue exposed to pulses of different amplitudes.

Keywords: magnetic resonance electrical impedance tomography, electrical conductivity, current density imaging, electroporation

(Some figures may appear in colour only in the online journal)

1. Introduction

Electroporation is a phenomenon caused by an electric field of adequate strength and duration externally applied to cells, that results in an increase of cell membrane permeability to various molecules, which otherwise are deprived of a transmembrane transport mechanism (Neumann *et al* 1982, Orlowski *et al* 1988, Tsong 1991, Sersa *et al* 1995, Mir *et al* 1999, Kotnik *et al* 2012). Cells can be exposed to an electric field by applying electric pulses generated by an electric pulse generator via electrodes. When electric parameters (number, shape, duration and repetition frequency of electric pulses and direction of electric field), electrode geometry and electrode positions are appropriately chosen and consequently cells are exposed to adequate electric field (Miklavcic *et al* 1998, 2006, Miklavcic and Towhidi 2010), permeabilization of the plasma membrane can be attained and the cell membrane reseals afterwards (Neumann *et al* 1982, Zimmermann 1982). Electroporation can thus be used to introduce various molecules into cells or to kill cells by using reversible or irreversible electroporation (Davalos *et al* 2005, Haberl *et al* 2013), respectively.

Monitoring of the electroporation process is one of the most important aspects of safe and efficient use of electroporation in clinical procedures such as electrochemotherapy (Marty *et al* 2006, Sersa and Miklavcic 2008, Miklavcic *et al* 2012) and nonthermal irreversible electroporation ablation (Garcia *et al* 2011, Rubinsky *et al* 2008, Neal *et al* 2013). As the membrane electroporation is a consequence of an induced transmembrane potential, which is directly proportional to the local electric field (Kotnik *et al* 2010), we proposed current density imaging (CDI) and magnetic resonance electrical impedance tomography (MREIT) techniques to determine the electric field distribution during electroporation (Kranjc *et al* 2011, 2012). CDI is a magnetic resonance imaging (MRI) method for acquiring current density distribution inside conductive samples by measuring magnetic field changes caused by applied current (Joy *et al* 1989, Scott *et al* 1991, Sersa *et al* 1994, Gamba and Delpy 1998), whereas tissue conductivity can be obtained by MREIT, a technique used for reconstruction of electrical conductivity inside a tissue by means of current density (Kwon *et al* 2002a, Woo *et al* 1994, Eybolu *et al* 2001, Kwon *et al* 2002a, Seo *et al* 2003b, Oh *et al* 2003). As the measurement of current density and electrical conductivity is performed during electric pulse delivery, the electric field distribution determined also takes into account changes which occur in tissue due to electroporation (Kranjc *et al* 2012, Essone Mezeme *et al* 2012).

Measurement of electrical properties of tissues affected by electroporation has already been suggested as an approach to assessing the effects of electroporation (Ivorra and Rubinsky 2007, Granot *et al* 2009, Ivorra *et al* 2009, Grafstrm *et al* 2006, Edd *et al* 2006). It has been demonstrated by measuring changes in electrical properties of cells (Huang and Rubinsky 1999), cell cultures (Pavlin *et al* 2005) and also tissues (Pliquett *et al* 1995, Pliquett and Prausnitz 2000, Davalos *et al* 2002, Cukjati *et al* 2007, Pliquett and Schoenbach 2009) undergoing electroporation. The most prominent technique for assessment of changes in electrical properties of electroporated tissues have been voltage–current measurement of applied pulses (Cukjati *et al* 2007) and electrical impedance tomography (EIT) (Ivorra and Rubinsky 2007, Granot *et al* 2009). The method of measuring voltage and current of applied pulses was primarily established for real time electroporation control through adjusting voltage amplitude of pulses for *in vivo* nonviral gene therapy (Cukjati *et al* 2007). However, assessed electrical conductivity lacks information on tissue heterogeneity, as it depends on electrode geometry and location. EIT is based on multiple electrode placement around the tissue, through which small currents are injected while multiple measurements of voltage are carried out on the tissue boundary. The electrical conductivity of the tissue can then be reconstructed using the finite element method (Holder 2004). EIT studies showed a correlation between treatment

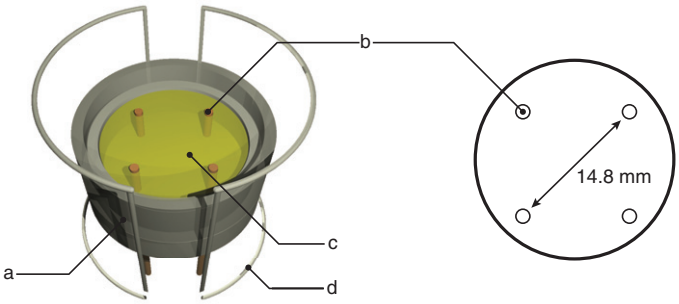

Figure 1. The container (a) used in the study was made of acrylic glass with four holes for electrodes (b). Either an agar phantom or liver tissue (c) was placed inside. The container was inserted in the radio-frequency (RF) probe (d). The distance between the active electrodes was 14.8 mm.

outcome and changes of electrical properties of tissue, as its conductivity increased by up to 180% after the treatment (Ivorra *et al* 2009). MREIT is in many aspects similar to EIT, as it is also used for reconstruction of conductivity images. The difference between the two techniques is in voltage and current measurements, which in EIT are limited to the boundaries of the measurement object, while in MREIT they cover the entire object, hence producing conductivity images with better spatial resolution.

Another benefit of measurement of electrical properties of tissues affected by electroporation would be a better characterization of numerical models of tissues in patient specific pre-treatment plans (Miklavcic *et al* 2010, Zupanic *et al* 2012, Neal *et al* 2012, Pavliha *et al* 2012). Namely, the local electric field in tissues is affected by applied electroporation pulses, which depend on local electrical conductivity, and vice versa electroporation increases the conductivity and consequently alters the electric field distribution (Sel *et al* 2005, Pavselj *et al* 2005). This makes it difficult to properly characterize the numerical model of the treated tissue, and therefore the pre-treatment plan cannot assure required coverage of the treated tissue with accurate electric field, as it relies mostly on the accuracy of the electrical conductivity of the treated tissue used in the numerical model (Kos *et al* 2010). As there is a lack of tissue specific experimental data on tissue properties for reliable patient specific pre-treatment planning, MREIT could be of significant help in determining more accurate values of electrical conductivity for various tissues undergoing electroporation treatment.

The aim of our study was to investigate and demonstrate the feasibility of the MREIT technique for assessment of conductivity images of tissues undergoing electroporation. Two objects were investigated: an agar phantom and *ex vivo* liver tissue. Both were exposed to short high-voltage pulses, as are normally used in electroporation clinical applications. No alteration of electrical conductivity was expected in the agar phantom, while increased conductivity was anticipated in the *ex vivo* liver tissue as a result of electroporation.

2. Material and methods

2.1. Measurement setup

All experiments were done in an acrylic glass container measuring 21 mm in diameter and 2 mm in height as shown in figure 1. The measurement object, either the agar phantom or the liver tissue, was placed inside the container in which needle electrodes were inserted through four holes located on the top of the container.

The container was placed inside the horizontal bore superconducting magnet together with the radio-frequency (RF) probe. Electrodes were connected to an electric pulse generator, which was triggered by an MRI control unit and synchronized with the CDI pulse sequence. A low-pass filter was also used to avoid RF disturbances in the NMR signal. All experiments were repeated three times.

The CDI method was used for acquiring electric current density when electric pulses were delivered to the measurement object. The obtained current density was then used for reconstruction of electrical conductivity using the MREIT J-substitution algorithm.

2.2. Agar phantom and liver tissue

Measurement of electrical conductivity during electroporation was performed on two objects: an agar phantom and *ex vivo* liver tissue. The agar phantom was made of agar powder (Kemika, Croatia), 0.9% NaCl saline solution (Braun, Germany) and distilled deionized water (Braun, Germany) in order to decrease the electrical conductivity of the agar mixture to the range of *ex vivo* liver tissue. *Ex vivo* measurement of electrical conductivity was done on fresh chicken liver tissue, that was obtained from a slaughterhouse (Perutnina Ptuj, Ptuj, Slovenia) which operates in accordance with Slovenian law.

Both measurement objects were sliced into cylindrical shapes measuring 21 mm in diameter and 2 mm in height and placed in the acrylic glass container. They were replaced with a fresh sample after each electroporation pulse delivery to ensure identical initial conditions in all electroporation experiments.

2.3. Electroporation protocol

Electroporation was performed by applying two sequences of four high-voltage electric pulses (eight pulses altogether) with a pulse duration of 100 μs, a pulse repetition frequency of 5 kHz and an amplitude U_e of either 500, 1000 or 1500 V. The electric pulses were delivered by a Cliniporator VITAE electric pulse generator (IGEA, Carpi, Italy) between two diagonal electrodes that were 14.8 mm apart. The electrodes were made of platinum–iridium, were cylindrically shaped and measured 1 mm in diameter. The voltage and current of the electric pulses were measured at the end of the last pulse with an oscilloscope (WavePro 7300A, LeCroy, USA) using a current probe (AP015, LeCroy, USA) and a high-voltage probe (PPE2KV, LeCroy, USA).

2.4. Magnetic resonance electrical impedance tomography (MREIT)

Electrical conductivity of agar phantoms and *ex vivo* liver tissue during electroporation was obtained by MREIT. MREIT is an MRI modality based on CDI for visualization of an electrical conductivity distribution inside a conductive sample.

CDI is an MRI method for acquiring the current density distribution inside conductive samples during the application of electric pulses (Joy *et al* 1989, Sersa *et al* 1994). The method is based on detecting magnetic field changes caused by applied electric current which is synchronized with the imaging sequence. Magnetic field changes cause a precession frequency shift that results in a precession phase shift (φ). The shift can be measured by the CDI imaging sequence (Sersa *et al* 1994):

$$\varphi = \gamma t_c B_z \tag{1}$$

where γ is the proton gyromagnetic ratio, t_c is the total duration of the applied electric pulses and B_z is the nonzero component of magnetic field in the direction of the static magnetic field and perpendicular to the direction of the imaging slice. The other two components (B_x, B_y)

were insignificant due to the measurement object geometry, in which currents were flowing predominantly in the direction perpendicular to the electrodes. When magnetic field changes were obtained by means of MRI, the current density distribution in measurement objects was calculated using Ampère's law (Maxwell 1865):

$$\mathbf{J}_{\mathrm{CDI}} = \frac{1}{\mu_0}\nabla \times \mathbf{B}. \tag{2}$$

A two-shot RARE (rapid acquisition with relaxation enhancement) current density MRI sequence was applied for mapping current density distributions during electroporation, as it allows faster magnetic field change mapping than the standard spin-echo based CDI (Sersa 2008). Parameters of the two-shot RARE imaging sequence were field of view 30 mm × 30 mm, imaging matrix 64 × 64, inter-echo delay 2.64 ms and echo time of the current encoding period 20 ms. MRI was performed on a Tecmag NMR spectrometer (Houston, TX) connected to an Oxford 2.35 T horizontal bore superconducting magnet (Abingdon, Oxfordshire, UK). The MRI system was equipped with Bruker microimaging accessories (Billerica, MA) with maximum gradients of 250 mTm^{-1}.

MREIT is a relatively new medical imaging modality based on numerical reconstruction of electrical conductivity inside a tissue by means of current density obtained by CDI (Woo *et al* 1994, Khang *et al* 2002, Seo and Woo 2011). The MREIT J-substitution algorithm was applied for reconstruction of electrical conductivity in the measurement objects (Kwon *et al* 2002b, Seo *et al* 2003a, Khang *et al* 2002). The algorithm is based on solving Laplace's equation inside a mathematical model of the measurement object Ω_{M} with the corresponding Neumann and Dirichlet boundary conditions on the measurement object outer boundary $\partial\Omega_{\mathrm{Mo}}$ and on the electrode boundary $\partial\Omega_{\mathrm{Me}+/-}$, respectively:

$$\nabla(\sigma_{\mathrm{M}}\nabla u) = 0 \quad \text{in} \quad \Omega_{\mathrm{M}} \tag{3}$$

$$\sigma_{\mathrm{M}}\frac{\partial u}{\partial n_{\mathrm{M}}} = 0 \quad \text{on} \quad \partial\Omega_{\mathrm{M}} \tag{4}$$

$$u = U_{\mathrm{e}} \quad \text{on} \quad \partial\Omega_{\mathrm{Me}+} \tag{5}$$

$$u = 0 \quad \text{on} \quad \partial\Omega_{\mathrm{Me}-} \tag{6}$$

where σ_{M} is the electrical conductivity of the measurement object and U_{e} is the voltage on the electrodes measured by the oscilloscope. Equations (3)–(6) are solved iteratively using the finite element method. After each iteration the solution u was used in

$$\sigma^*_{\mathrm{M}} = \frac{|\mathbf{J}_{\mathrm{CDI}}|}{|\nabla u|} \tag{7}$$

where σ^*_{M} is the new conductivity and $\mathbf{J}_{\mathrm{CDI}}$ is the current density obtained by the CDI method. The iterative scheme lasts until the relative difference between two successive σ_{M} values is negligible.

All equations were solved using the finite element method with the numerical computational environment MATLAB 2013a (MathWorks, Natick, MA) on a desktop PC (Windows 7, 2.66 GHz, 4 GB RAM).

2.5. Analysis of obtained electrical conductivity

The obtained electrical conductivity was analyzed for each applied voltage U_{e} in region of interest Ω_{MROI} located inside the mathematical model of the measurement object Ω_{M} as shown in figure 2. Ω_{MROI} enclosed an area where the electric field was the highest and the largest alteration of electrical conductivity due to electroporation was expected (Miklavcic *et al* 2000).

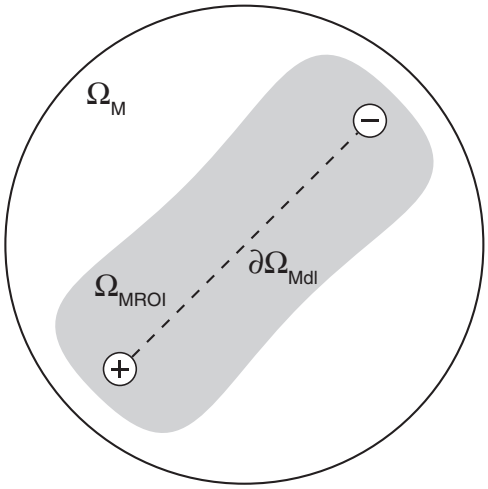

Figure 2. A mathematical model of the measurement object Ω_M. The electrical conductivity was analyzed inside region of interest Ω_{MROI} and along the diagonal line between the electrodes $\partial\Omega_{Mdl}$.

The electrical conductivity was also evaluated across the measurement object by determining the mean value of the conductivity $\overline{\sigma_{Mdl}}$ along the diagonal line between the electrodes $\partial\Omega_{Mdl}$. The Student t-test was used to evaluate the statistical significance of differences between obtained electrical conductivities. All results were analyzed and statistically described using the commercial software MATLAB 2013a (MathWorks, Natick, MA) and its statistics toolbox.

3. Results

When electric pulses were delivered to the measurement object, electric current density was established inside and acquired by the CDI method. The current density distribution was then applied to the MREIT J-substitution algorithm for reconstruction of electrical conductivity. Electrical conductivities of both measurement objects exposed to electric pulses of different amplitudes (U_e = 500, 1000, 1500 V) within Ω_{MROI} are shown in figure 3.

No detectable changes in electrical conductivity were observed in Ω_{MROI} when agar phantoms were exposed to pulses of 500, 1000 and 1500 V except in the region close to the electrodes. Similarly, no changes were measured in Ω_{MROI} in liver tissue exposed to pulses with an amplitude of 500 V. Changes in electrical conductivity started to appear when the pulse amplitude was increased to 1000 V. Furthermore, the greatest change of conductivity was detected when liver tissue was exposed to pulses with the highest amplitude of 1500 V. Mean values of the conductivity along the diagonal line between the electrodes $\partial\Omega_{Mdl}$ for both measurement objects as a function of applied amplitude of electric pulses are shown in figure 4. Differences between mean values of electrical conductivity of agar phantoms exposed to pulses with amplitudes of 500, 1000 and 1500 V were not statistically significant ($p > 0.01$). An increase of 1.5 and 37.1 m Sm^{-1} was measured when comparing mean values of electrical conductivity in liver tissue exposed to pulses with amplitudes of 500 V with mean values of electrical conductivity in liver tissue exposed to pulses with amplitudes of 1000 and 1500 V, respectively. These differences were statistically significant ($p < 0.01$).

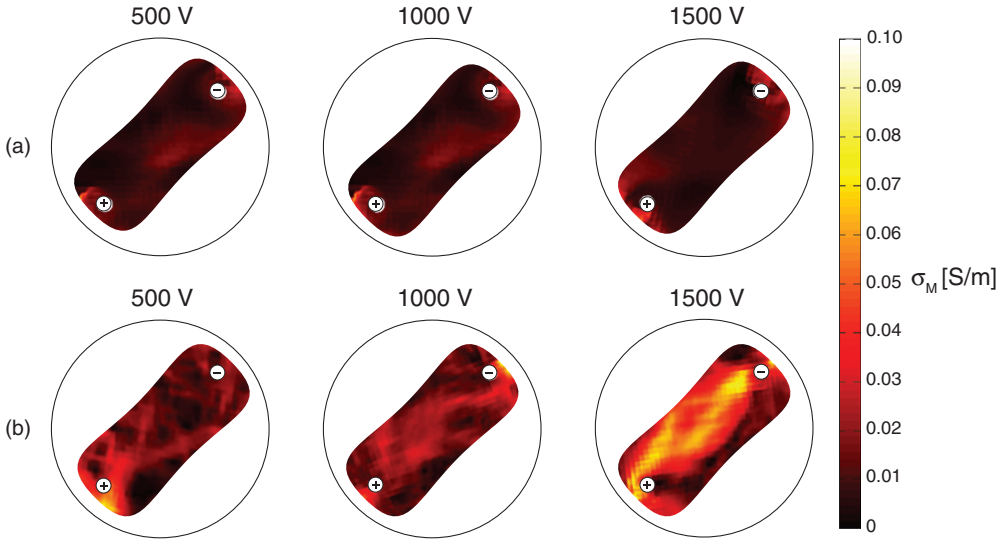

Figure 3. Electrical conductivities of (a) agar phantom and (b) liver tissue exposed to electric pulses of different amplitudes (U_e = 500, 1000, 1500 V). Electric pulses were delivered between two needle electrodes (marked with + and −). Each image of the measured object is a crop of the field of view.

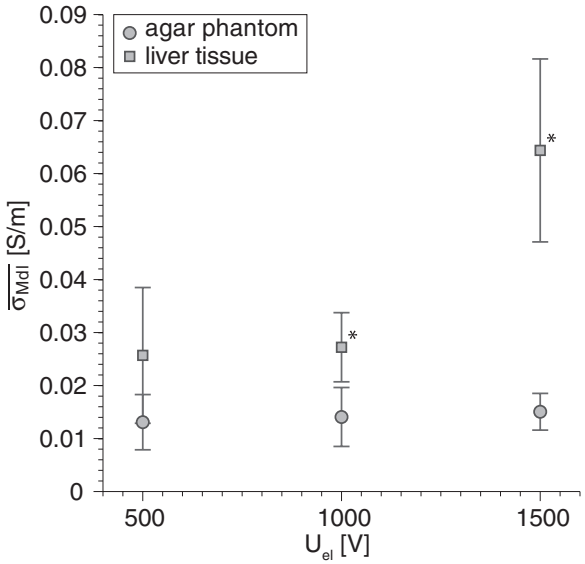

Figure 4. Mean values of electrical conductivity ($\overline{\sigma_{\mathrm{Mdl}}} \pm$ STD) along the diagonal line between the electrodes $\partial\Omega_{\mathrm{Mdl}}$ for an agar phantom and liver tissue exposed to electric pulses of different amplitudes (U_e = 500, 1000, 1500 V). $*$ denotes statistically significant difference ($p < 0.01$).

Table 1. Electric current at the end of the last pulse measured with the oscilloscope during pulse delivery for agar phantoms (I_{agar}) and liver tissue (I_{liver}). Results are presented as means ± standard deviations.

	U_e (V)		
	500	1000	1500
I_{agar} (A)	0.07 ± 0.02	0.15 ± 0.03	0.22 ± 0.02
I_{liver} (A)	0.16 ± 0.02	0.32 ± 0.08	0.67 ± 0.18

Electric currents measured with a current probe during application of electric pulses are presented in table 1 for agar phantoms and liver tissue exposed to pulses of all applied amplitudes.

4. Discussion

The aim of this study was to investigate and demonstrate the feasibility of the MREIT technique for assessment of conductivity images of tissues undergoing electroporation. The investigation was carried out on agar phantoms and *ex vivo* liver tissue that were subject to short high-voltage pulses, as are normally used in electroporation clinical applications. Different amplitudes of pulses were used in separate experiments to evaluate the feasibility of the proposed method to detect electrical conductivity changes of tissue.

As expected, no significant change of electrical conductivity was detected in agar phantoms exposed to pulses of all applied amplitudes. This was expected since agar lacks cell structure and therefore could not be affected by electroporation. In the region close to the electrodes there was a detectable conductivity increase as can be seen in figure 3. However, this was not a consequence of electroporation but of the electrodes, which caused distortions in the magnetic field and significant susceptibility artifacts in acquired phase images. Similar distortions in the magnetic field were also detected in liver tissue exposed to electric pulses. This presents a limitation to the MREIT approach of measuring electrical conductivity during electroporation, as it is not able to assess conductivity changes in the region close to the electrodes. Nevertheless, the region of interest of electroporation treatments is focused in the area between the electrodes and away from the electrodes, i.e. not in the immediate vicinity of the electrodes, where the highest electric field is established.

Significant differences can be observed in figure 3 when comparing changes of conductivity in agar phantoms with those in liver tissue. Furthermore, considerable differences can also be seen when comparing changes of conductivity within results of liver tissue exposed to pulses of different amplitudes. No conductivity change was, as in agar phantoms, still detected in liver tissue exposed to pulses with the amplitude of 500 V. A conductivity increase in liver tissue started to appear when the amplitude was increased to 1000 V. As they were located in regions away from the electrodes, detected conductivity changes could not be a consequence of magnetic field distortions due to the electrodes, but were rather a result of local tissue electroporation. This is even more evident in liver tissue exposed to pulses with the amplitude of 1500 V. Here, electrical conductivity increased by a factor of ∼1.5 in the middle of Ω_{MROI}, whereas in some regions it almost doubled. A similar nonlinear increase can be observed when comparing electric currents in liver tissue exposed to pulses with an amplitude of 1000 and 1500 V in table 1. Conductivity alterations are even more explicitly shown in figure 4, where electrical conductivity was evaluated along the diagonal line $\partial\Omega_{Mdl}$, which extended through the area where the applied electric field was the highest and the

electroporation process most efficient. Similar observations were also previously reported in studies employing EIT (Ivorra *et al* 2009) and voltage–current measurement of applied pulses (Cukjati *et al* 2007), where the conductivity of *in vivo* tissue increased by a factor of ∼1.5 and ∼2.1 when electric fields of the same magnitudes as used in this study were applied, respectively.

Different attempts to assess changes of tissue electrical properties that occur during electroporation have already been proposed, as mentioned in the introduction. Both the voltage–current measurement approach and EIT were successfully applied and showed an increase of electrical conductivity of tissue exposed to short high-voltage electric pulses. Unfortunately, there have been no reports on further development of the methods or on new results in recent times. On the other hand, new approaches to assessing the effects of electroporation have been introduced. They are all based on standard medical imaging procedures such as MRI (Hjouj *et al* 2012, Mahmood *et al* 2011, Zhang *et al* 2010, Rossmeisl *et al* 2014) and ultrasound (Lee *et al* 2007). The proposed methods are still focused solely on irreversible electroporation, where immediate changes of tissue properties can be detected by comparing images of different modalities acquired before and after application of pulses. Assessing changes of tissue properties during reversible electroporation is however a more demanding task, since there are no immediate visible physical changes in treated tissue. There are structural changes, which are reflected in diffusion-weighted images (Mahmood *et al* 2011), but they can only be detected after electric pulse delivery. Nevertheless, electrical conductivity is one of the known tissue properties which changes during reversible as well as in irreversible electroporation of tissue (Ivorra *et al* 2009). Therefore, different electroporation treatments could be monitored efficiently by assessing changes of conductivity in tissue during electroporation using MREIT or EIT. Furthermore, current density distribution is also obtained in addition to electrical conductivity with MREIT. This enables reconstruction of electric field distribution in tissue, the most important determinant of the electroporation process (Kotnik *et al* 2010).

As the measurement of electrical conductivity is performed during pulse delivery, the determined conductivity image takes into account all existing heterogeneities and changes which occur in tissue due to electroporation. Moreover, a single two-shot RARE CDI sequence takes about 20 s to acquire the current density distribution and the MREIT J-substitution algorithm an additional few seconds for reconstruction of electrical conductivity, but this could be further reduced. This makes CDI and MREIT capable of near real time monitoring of changes of electrical conductivity which occur during electroporation, as they can then be determined in a few tens of seconds after the beginning of pulse delivery. However, there is a limitation with the existing two-shot RARE CDI sequence, as it requires an application of at least two electric pulses with a delay of approximately 15 s between them in order to deliver complete current density information. This currently puts a frequency limitation on CDI, although hopefully future improvements of CDI algorithms and MRI scanners will enable us to reduce the required delay between applied pulses.

5. Conclusion

We have described and experimentally investigated the assessment of conductivity changes of tissues undergoing electroporation by means of MREIT on agar phantoms and liver tissue. The results show no significant change of electrical conductivity in agar phantoms exposed to pulses at all amplitudes used, but considerable increase of conductivity in liver tissue exposed to pulses of different amplitudes. This suggests that MREIT can indeed be used for detecting

electrical conductivity changes that occur in tissue exposed to short high-voltage pulses, and that the proposed method can be used for assessment and prediction of the electroporation effect on tissue.

Acknowledgments

This study was supported by the Slovenian Research Agency (ARRS) and conducted within the scope of the Electroporation in Biology and Medicine European Associated Laboratory (LEA-EBAM). This manuscript is a result of the networking efforts of the COST Action TD1104 (www.electroporation.net).

References

Cukjati D, Batiuskaite D, Andr F, Miklavcic D and Mir L M 2007 Real time electroporation control for accurate and safe *in vivo* non-viral gene therapy *Bioelectrochemistry* **70** 501–7

Davalos R V, Mir L M and Rubinsky B 2005 Tissue ablation with irreversible electroporation *Ann. Biomed. Eng.* **33** 223–31

Davalos R V, Rubinsky B and Otten D M 2002 A feasibility study for electrical impedance tomography as a means to monitor tissue electroporation for molecular medicine *IEEE Trans. Biomed. Eng.* **49** 400–3

Edd J F, Horowitz L, Davalos R V, Mir L M and Rubinsky B 2006 *In vivo* results of a new focal tissue ablation technique: irreversible electroporation *IEEE Trans. Biomed. Eng.* **53** 1409–15

Essone Mezeme M, Kranjc M, Bajd F, Sersa I, Brosseau C and Miklavcic D 2012 Assessing how electroporation affects the effective conductivity tensor of biological tissues *Appl. Phys. Lett.* **101** 213702

Eybolu B M, Birgl O and Ider Y Z 2001 A dual modality system for high resolution—true conductivity imaging *ICEBI: Proc. 11th Int. Conf. on Electrical Bioimpedance* pp 409–13

Gamba H and Delpy D 1998 Measurement of electrical current density distribution within the tissues of the head by magnetic resonance imaging *Med. Biol. Eng. Comput.* **36** 165–70

Garcia P A, Pancotto T, Rossmeisl J H, Henao-Guerrero N, Gustafson N R, Daniel G B, Robertson J L, Ellis T L and Davalos R V 2011 Non-thermal irreversible electroporation (N-TIRE) and adjuvant fractionated radiotherapeutic multimodal therapy for intracranial malignant glioma in a canine patient *Technol. Cancer Res. Treat.* **10** 73–83 (PMID: 21214290)

Grafstrm G, Engstrm P, Salford L G and Persson B R 2006 99mTc-DTPA uptake and electrical impedance measurements in verification of *in vivo* electropermeabilization efficiency in rat muscle *Cancer Biother. Radiopharm.* **21** 623–35

Granot Y, Ivorra A, Maor E and Rubinsky B 2009 *In vivo* imaging of irreversible electroporation by means of electrical impedance tomography *Phys. Med. Biol.* **54** 4927–43

Haberl S, Miklavcic D, Sersa G, Frey W and Rubinsky B 2013 Cell membrane electroporation: part 2. The applications *IEEE Electr. Insul. Mag.* **29** 29–37

Hjouj M, Last D, Guez D, Daniels D, Sharabi S, Lavee J, Rubinsky B and Mardor Y 2012 MRI study on reversible and irreversible electroporation induced blood brain barrier disruption *PLoS One* **7** e42817

Holder D S (ed) 2004 *Electrical Impedance Tomography: Methods, History and Applications* 1st edn (London: Taylor and Francis)

Huang Y and Rubinsky B 1999 Micro-electroporation: improving the efficiency and understanding of electrical permeabilization of cells *Biomed. Microdevices* **2** 145–50

Ivorra A, Al-Sakere B, Rubinsky B and Mir L M 2009 *In vivo* electrical conductivity measurements during and after tumor electroporation: conductivity changes reflect the treatment outcome *Phys. Med. Biol.* **54** 5949–63

Ivorra A and Rubinsky B 2007 *In vivo* electrical impedance measurements during and after electroporation of rat liver *Bioelectrochemistry* **70** 287–95

Joy M, Scott G and Henkelman M 1989 *In vivo* detection of applied electric currents by magnetic-resonance imaging *Magn. Reson. Imaging* **7** 89–94

Khang H S, Lee B I, Oh S H, Woo E J, Lee S Y, Cho M Y, Kwon O, Yoon J R and Seo J K 2002 J-substitution algorithm in magnetic resonance electrical impedance tomography (MREIT): phantom experiments for static resistivity images *IEEE Trans. Med. Imaging* **21** 695–702

Kos B, Zupanic A, Kotnik T, Snoj M, Sersa G and Miklavcic D 2010 Robustness of treatment planning for electrochemotherapy of deep-seated tumors *J. Membr. Biol.* **236** 147–53

Kotnik T, Kramar P, Pucihar G, Miklavcic D and Tarek M 2012 Cell membrane electroporation: part 1. The phenomenon *IEEE Electr. Insul. Mag.* **28** 14–23

Kotnik T, Pucihar G and Miklavcic D 2010 Induced transmembrane voltage and its correlation with electroporation-mediated molecular transport *J. Membr. Biol.* **236** 3–13

Kranjc M, Bajd F, Sersa I and Miklavcic D 2011 Magnetic resonance electrical impedance tomography for monitoring electric field distribution during tissue electroporation *IEEE Trans. Med. Imaging* **30** 1771–8

Kranjc M, Bajd F, Sersa I, Woo E J and Miklavcic D 2012 *Ex vivo* and *in silico* feasibility study of monitoring electric field distribution in tissue during electroporation based treatments *PLoS One* **7** e45737

Kwon O, Lee J and Yoon J 2002a Equipotential line method for magnetic resonance electrical impedance tomography *Inverse Problems* **18** 1089–100

Kwon O, Woo E, Yoon J and Seo J 2002b Magnetic resonance electrical impedance tomography (MREIT): simulation study of J-substitution algorithm *IEEE Trans. Biomed. Eng.* **49** 160–7

Lee E W, Loh C T and Kee S T 2007 Imaging guided percutaneous irreversible electroporation: ultrasound and immunohistological correlation *Technol. Cancer Res. Treat.* **6** 287–94

Mahmood F, Hansen R H, Agerholm-Larsen B, Jensen K S, Iversen H K and Gehl J 2011 Diffusion-weighted MRI for verification of electroporation-based treatments *J. Membr. Biol.* **240** 131–8

Marty M *et al* 2006 Electrochemotherapy—an easy, highly effective and safe treatment of cutaneous and subcutaneous metastases: results of ESOPE (European Standard Operating Procedures of Electrochemotherapy) study *Eur. J. Cancer Suppl.* **4** 3–13

Maxwell J C 1865 A dynamical theory of the electromagnetic field *Phil. Trans. R. Soc. Lond.* **155** 459–512

Miklavcic D, Beravs K, Semrov D, Cemazar M, Demsar F and Sersa G 1998 The importance of electric field distribution for effective *in vivo* electroporation of tissues *Biophys. J.* **74** 2152–8

Miklavcic D, Corovic S, Pucihar G and Pavselj N 2006 Importance of tumour coverage by sufficiently high local electric field for effective electrochemotherapy *Eur. J. Cancer Suppl.* **4** 45–51

Miklavcic D, Semrov D, Mekid H and Mir L M 2000 A validated model of *in vivo* electric field distribution in tissues for electrochemotherapy and for DNA electrotransfer for gene therapy *Biochim. Biophys. Acta* **1523** 73–83

Miklavcic D, Sersa G, Brecelj E, Gehl J, Soden D, Bianchi G, Ruggieri P, Rossi C, Campana L and Jarm T 2012 Electrochemotherapy: technological advancements for efficient electroporation-based treatment of internal tumors *Med. Biol. Eng. Comput.* **50** 1213–25

Miklavcic D, Snoj M, Zupanic A, Kos B, Cemazar M, Kropivnik M, Bracko M, Pecnik T, Gadzijev E and Sersa G 2010 Towards treatment planning and treatment of deep-seated solid tumors by electrochemotherapy *Biomed. Eng. Online* **9** 10

Miklavcic D and Towhidi L 2010 Numerical study of the electroporation pulse shape effect on molecular uptake of biological cells *Radiol. Oncol.* **44** 34–41

Mir L M, Bureau M F, Gehl J, Rangara R, Rouy D, Caillaud J M, Delaere P, Branellec D, Schwartz B and Scherman D 1999 High-efficiency gene transfer into skeletal muscle mediated by electric pulses *Proc. Natl Acad. Sci. USA* **96** 4262–7

Neal R E, Garcia P A, Robertson J L and Davalos R V 2012 Experimental characterization and numerical modeling of tissue electrical conductivity during pulsed electric fields for irreversible electroporation treatment planning *IEEE Trans. Biomed. Eng.* **59** 1076–85

Neal R E, Kavnoudias H, Cheung W, Golebiowski B, McLean C A and Thomson K R 2013 Hepatic epithelioid hemangioendothelioma treated with irreversible electroporation and antibiotics *J. Clin. Oncol.* **27** 422–6

Neumann E, Schaeferridder M, Wang Y and Hofschneider P 1982 Gene transfer into mouse lyoma cells by electroporation in high electric-fields *EMBO J.* **1** 841–5

Oh S H, Lee B I, Woo E J, Lee S Y, Cho M H, Kwon O and Seo J K 2003 Conductivity and current density image reconstruction using harmonic Bz algorithm in magnetic resonance electrical impedance tomography *Phys. Med. Biol.* **48** 3101–16

Orlowski S, Belehradek J, Paoletti C and Mir L M 1988 Transient electropermeabilization of cells in culture. Increase of the cytotoxicity of anticancer drugs *Biochem. Pharmacol.* **37** 4727–33

Pavliha D, Kos B, Zupanic A, Marcan M, Sersa G and Miklavcic D 2012 Patient-specific treatment planning of electrochemotherapy: procedure design and possible pitfalls *Bioelectrochemistry* **87** 265–73

Pavlin M, Kanduser M, Rebersek M, Pucihar G, Hart F X, Magjarevic R and Miklavcic D 2005 Effect of cell electroporation on the conductivity of a cell suspension *Biophys. J.* **88** 4378–90

Pavselj N, Bregar Z, Cukjati D, Batiuskaite D, Mir L and Miklavcic D 2005 The course of tissue permeabilization studied on a mathematical model of a subcutaneous tumor in small animals *IEEE Trans. Biomed. Eng.* **52** 1373–81

Pliquett U, Langer R and Weaver J C 1995 Changes in the passive electrical properties of human stratum corneum due to electroporation *Biochim. Biophys. Acta* **1329** 111–21

Pliquett U and Prausnitz M R 2000 Electrical impedance spectroscopy for rapid and noninvasive analysis of skin electroporation *Methods Mol. Med.* **37** 377–406

Pliquett U and Schoenbach K 2009 Changes in electrical impedance of biological matter due to the application of ultrashort high voltage pulses *IEEE Trans. Dielectr. Electr. Insul.* **16** 1273–9

Rossmeisl J, Garcia P, Daniel G, Bourland J, Debinski W, Dervisis N and Klahn S 2014 Invited review—neuroimaging response assessment criteria for brain tumors in veterinary patients *Vet. Radiol. Ultrasound* **55** 115–32

Rubinsky J, Onik G, Mikus P and Rubinsky B 2008 Optimal parameters for the destruction of prostate cancer using irreversible electroporation *J. Urol.* **180** 2668–74

Scott G, Joy M, Armstrong R and Henkelman R 1991 Measurement of nonuniform current-density by magnetic-resonance *IEEE Trans. Med. Imaging* **10** 362–74

Sel D, Cukjati D, Batiuskaite D, Slivnik T, Mir L and Miklavcic D 2005 Sequential finite element model of tissue electropermeabilization *IEEE Trans.Biomed. Eng.* **52** 816–27

Seo J, Kwon O, Lee B and Woo E 2003a Reconstruction of current density distributions in axially symmetric cylindrical sections using one component of magnetic flux density: computer simulation study *Physiol. Meas.* **24** 565–77

Seo J K and Woo E J 2011 Magnetic resonance electrical impedance tomography (MREIT) *SIAM Rev.* **53** 40

Seo J K, Yoon J R, Woo E J and Kwon O 2003b Reconstruction of conductivity and current density images using only one component of magnetic field measurements *IEEE Trans. Biomed. Eng.* **50** 1121–4

Sersa G, Cemazar M and Miklavcic D 1995 Antitumor effectiveness of electrochemotherapy with cis-diamminedichloroplatinum(II) in mice *Cancer Res.* **55** 3450–5

Sersa G and Miklavcic D 2008 Electrochemotherapy of tumours *J. Visual. Exp.* **22** e1038

Sersa I 2008 Auxiliary phase encoding in multi spin-echo sequences: application to rapid current density imaging *J. Magn. Reson.* **190** 86–94

Sersa I, Jarh O and Demsar F 1994 Magnetic resonance microscopy of electric currents *J. Magn. Reson. Ser.* A **111** 93–99

Tsong T Y 1991 Electroporation of cell membranes *Biophys. J.* **60** 297–306

Woo E J, Lee S Y and Mun C W 1994 Impedance tomography using internal current density distribution measured by nuclear magnetic resonance *Proc. SPIE* **2299** 377–85

Zhang Y, Guo Y, Ragin A B, Lewandowski R J, Yang G Y, Nijm G M, Sahakian A V, Omary R A and Larson A C 2010 MR imaging to assess immediate response to irreversible electroporation for targeted ablation of liver tissues: preclinical feasibility studies in a rodent model1 *Radiology* **256** 424–32

Zimmermann U 1982 Electric field-mediated fusion and related electrical phenomena *Biochim. Biophys. Acta* **694** 227–77

Zupanic A, Kos B and Miklavcic D 2012 Treatment planning of electroporation-based medical interventions: electrochemotherapy, gene electrotransfer and irreversible electroporation *Phys. Med. Biol.* **57** 5425–40